BIROn - Birkbeck Institutional Research Online

Cassini CAPS-ELS observations of negative ions in Titan's ionosphere: Trends of density with altitude

A. Wellbrock,[1,2] A. J. Coates,[1,2] G. H. Jones,[1,2] G. R. Lewis,[1,2] and J. H. Waite[3]

[1] Observations with the Electron Spectrometer sensor of the Cassini Plasma Spectrometer (CAPS-ELS) have revealed the existence of negative ions in Titan's ionosphere. Negative ions are observed during encounters whenever the instrument points in the ram direction at altitudes 950–1400 km. Complex hydrocarbon and nitrile chemical processes are believed to take place which play a role in haze formation. The heaviest ions observed so far have masses up to 13,800 amu/q. Using data from 34 Titan encounters, we show for the first time negative ion density trends of different mass groups, including total densities, with altitude. We determine peak densities and the associated altitudes at which they are observed and the highest altitudes at which individual mass groups are found.
Citation: Wellbrock, A., A. J. Coates, G. H. Jones, G. R. Lewis, and J. H. Waite (2013), Cassini CAPS-ELS observations of negative ions in Titan's ionosphere: Trends of density with altitude, *Geophys. Res. Lett.*, *40*, 4481–4485, doi:10.1002/grl.50751.

1. Introduction

[2] Titan is Saturn's largest moon with a radius of 2575 km. Under standard solar wind dynamic conditions, in addition to solar radiation, its extensive nitrogen- and methane-based atmosphere is exposed to Saturn's magnetospheric plasma. The upper layers of the moon's atmosphere form an extensive ionosphere whose characteristics have been probed by the Cassini spacecraft since 2004 [e.g., *Sittler et al.*, 2010; *Cravens et al.*, 2010].

[3] Although most space plasmas are dominated by positive ions, negative ions are plentiful and important for understanding the chemistry in several contexts. They have been observed remotely in interstellar clouds [e.g., *Herbst*, 1981; *Bruecken et al.*, 2007], in situ at comets [*Chaizy et al.*, 1991], in the Earth's ionosphere [e.g., *Hargreaves*, 1992], and more recently also at Saturn's moon Enceladus using the Cassini Plasma Spectrometer (CAPS) Electron Spectrometer (ELS) [*Coates et al.*, 2010a, 2010b].

[4] Observations of negative ions at Titan were first reported by *Coates et al.* [2007] and *Waite et al.* [2007] at altitudes ~1000 km and above. Negative ions were completely unexpected at these heights before Cassini's arrival in the Saturn system. They were only expected at lower altitudes and in the cosmic ray induced ionosphere below 200 km [e.g., *Hunten et al.*, 1984; *Borucki et al.*, 2006]. *Waite et al.* [2007, 2010] and *Coates et al.* [2007] explain that the very high-mass negative ions may not be true molecules but most likely aerosol monomers formed by the clumping of smaller molecules. *Coates et al.* [2009] showed that the highest mass ions occur at the lowest altitudes. *Sittler et al.* [2009] proposed that the detected heavy ions may be seed particles for aerosols at much lower altitudes. Recently, agglomeration due to charging [*Michael et al.*, 2011] or chemical processes [*Lavvas et al.*, 2013] was proposed to constrain the production process of the high-mass ions.

2. Data Analysis

[5] CAPS-ELS is a hemispherical top-hat electrostatic analyzer which was designed to measure the flux of electrons as a function of energy per charge and direction of arrival [*Young et al.*, 2004]. CAPS is located on an actuator which increases its field of view. A typical Titan flyby (T26) with negative ion detections is shown in Figure 1. Most negative ion observations in ELS spectrograms were obtained when CAPS was actuating and can be identified as vertical "spikes" such as the one inside region "B" in Figure 1. These are detected at energies ≤ 2550 eV, with the lowest energy at a few eV. Higher energy ions are generally only detected at lower altitudes, i.e., near closest approach on low encounters (e.g., 1000 km). At higher altitudes (e.g., 1300 km), the spikes cover a smaller energy range and the signatures generally look like that inside region "A" in Figure 1. Observations at intermediate altitudes can be seen between the two regions and also after B on the outbound leg. We refer to events such as those inside regions A and B as negative ion signatures. Each signature is a collection of peaks in the energy spectrum.

[6] The cold negative ions are detected only when the instrument points in the ram direction as described by *Coates et al.* [2007]; we do not observe negative ions between the spike-shaped structures because the instrument is actuating and at these times, the instrument does not point in the ram direction. We can determine the negative ion mass by assuming the observed ram energy as the kinetic energy of the ions and the spacecraft velocity as the relative speed for each encounter [*Coates et al.*, 2007]. This is reasonable as these cold ions are expected to have much lower thermal and convective velocities compared to the spacecraft velocity in the same Titan frame. Using this method, the mass of a singly charged negative ion is given by $m = 2E/v^2$, where
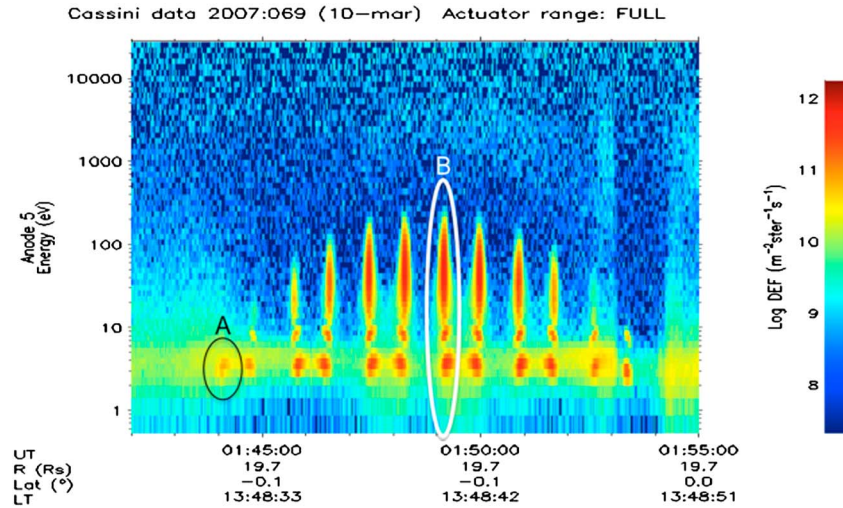

Figure 1. T26 electron spectrogram. Regions A and B indicate examples of negative ion signatures.

E is the observed (spacecraft potential corrected) energy and v is the spacecraft velocity. Converting mass and energy units to amu/q and eV, respectively, $m_{amu/q} = cE_{eV}$, where c is the conversion factor $c = 1.93 \times 10^8 / v^2$. The spacecraft velocity during encounters discussed here varies between $5.96 \, \text{km s}^{-1}$ and $6.35 \, \text{km s}^{-1}$, and an example value for c with $v = 6 \, \text{km s}^{-1}$ is 5.36. The highest mass observed in Titan's ionosphere to date is 13,800 amu/q [*Coates et al.*, 2009]. It should be noted that ELS measures E/q; hence, if an ion carries multiple charges, then the mass would be larger. Assuming that each negative ion carries a single charge, each negative ion signature in ELS spectrograms essentially represents a mass spectrum.

[7] *Coates et al.* [2007] describe six mass groups which were determined from recurring peaks in the mass spectra (not shown). Using a larger number of flybys, we have since updated these mass group boundaries; they are slightly narrower and a broad high-mass peak that is observed during some flybys led to the addition of a seventh group which includes masses of 625 amu/q and above (Table 1). *Vuitton et al.* [2009] presented the first chemical model of Titan's upper atmosphere to include negative ions. They compared the model results with CAPS-ELS data and identified mass groups 1–3 as CN^-, C_3N^-, and C_5N^-, respectively. C_4H^- may also contribute to mass group 3 above 1100 km. *Coates et al.* [2009] used CAPS-ELS data to investigate at which altitudes, latitudes, and solar zenith angles the highest

mass negative ions are found. We continue this work on negative ion observations with the first detailed density trend study of the different mass groups. In this study, we use negative ion signatures that have been detected with CAPS-ELS during 34 encounters between the first Titan flyby and T71 (7 July 2010). They are detected if (i) the encounter is low enough ($\sim < 1400 \, \text{km}$) and (ii) the instrument points in the ram direction.

[8] A number of data-processing routines specifically designed for the analysis of negative ions with CAPS-ELS such as inter-anode scaling and electron background subtraction are required. The electron background is removed using another anode which does not point in the ram direction and therefore does not observe negative ions. After data processing, the negative ion counts can be used to calculate the negative ion number density. The detailed method will be published as a separate study with focus on the data-processing method. To correct for negative spacecraft potential, RPWS (Radio and Plasma Wave Science) spacecraft potential data were used (A. Ågren, personal communication, 2012).

[9] To calculate negative ion densities from the processed negative ion counts, we assume that the count rate multiplied by the ion charge represent a current of ions in the ram direction:

$$n = \frac{C}{A\varepsilon v}$$

where n is the negative ion density, C is the count rate, $A = 0.33 \, \text{cm}^2$ is the effective area of the instrument estimated from aperture size and ground calibration data, ε is the estimated microchannel plate (MCP) efficiency for ions at this bias voltage, and v is the spacecraft velocity [*Coates et al.*, 2007]. It is difficult to estimate ε because negative ions were not expected at Cassini flyby altitudes; therefore, the CAPS-ELS MCPs were never tested or calibrated on the ground using negative ions. *Coates et al.* [2007] used an MCP efficiency of 0.05 to calculate total negative ion densities. From investigations of energy- and mass-dependent ion detection efficiencies performed by, e.g., *Fraser* [2002], this efficiency value appears adequate in the energy and mass range of interest here and we continue its use in this study. However, the uncertainty on the MCP efficiency may be as large as 50%. The resulting uncertainty on the ion densities

Table 1. Comparison of Mass Groups From *Coates et al.* [2007] and the Updated Mass Groups[a]

Mass Group	Mass Range (amu/q)		Reference Density (cm^{-3})
	Coates et al. [2007]	This study	
1	10–30	12–30	5.3
2	30–50	30–55	3.5
3	50–80	55–95	0.5
4	80–110	95–130	0.3
5	110–200	130–190	0.1
6	200+	190–625	0.2
7		625+	0.2
Total			9.7

[a]The right-hand column shows the reference density (see text) for all mass groups and total density at the bottommost row.

Table 2. Summary of Negative Ion Density Altitude Trends

Mass Group	Mass Range (amu/q)	Maximum Density (cm^{-3})[a]	Flyby of Max Density[b]	Altitude at Max Density (km)[c]	Peak Average Altitude (km)[d]	Reference Altitude (km)[e]
1	12–30	112	T43	1049	1066	1367
2	30–55	92	T41	1030	1061	1355
3	55–95	36	T43	1018	1056	1336
4	95–130	43	T41	1030	1029	1285
5	130–190	83	T29	1017	1014	1263
6	190–625	593	T23	1004	1000	1205
7	625+	331	T30	980	984	1098
Total[f]		948	T23	1004	1021	1355

[a]The "maximum density" column shows the maximum recorded density of all flybys for that mass group.
[b]The "flyby of max density" column shows during which flyby this maximum density was observed.
[c]The "altitude at max density" column shows the altitude at which the maximum density was observed.
[d]"Peak average altitude" shows the average of the altitudes at which densities peak during individual flybys.
[e]The rightmost column shows the reference altitude which is the maximum altitude at which negative ions in that mass group are observed above the mass group's reference density.
[f]The bottommost row shows total densities.

is 50% of the values shown on the plots, which is the dominant uncertainty. Due to this value, we suggest that the calculated negative ion densities are mainly useful in relative terms within the mass groups. The uncertainty due to the

MCP efficiency is mostly systematic in nature; hence, comparing density ranges within the group is accurate. An additional complication is that the response is likely to vary as a function of ion mass. We hence also suggest that the
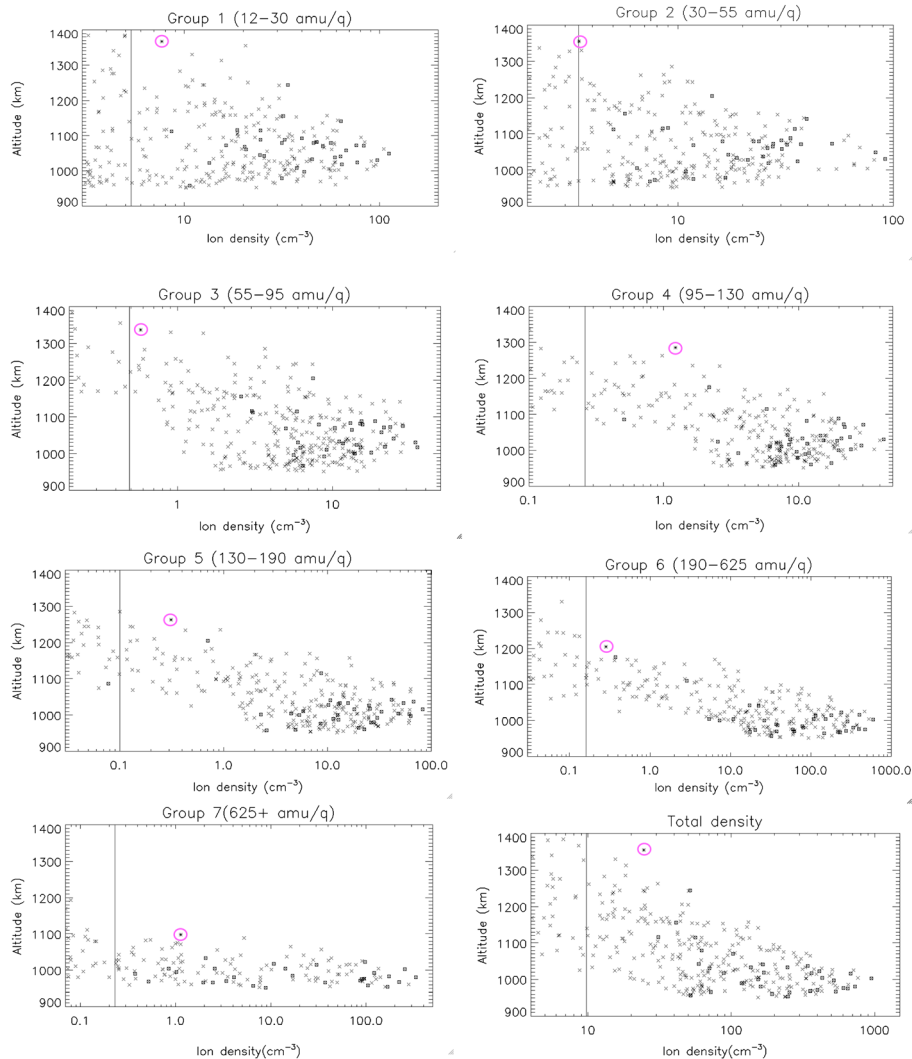

Figure 2. Altitude-density plots of mass groups 1 to 7 and total density. The vertical lines indicate the reference density. The asterisk highlighted by the pink circle for each mass group indicates the data point determining the reference altitude (see Table 2). The squares show the peak density for each flyby.

absolute values of the densities should not be compared directly, especially between mass groups with high-mass differences. In addition, we note that the energy bins of CAPS-ELS are spaced quasi-logarithmically and different mass groups cover different mass ranges. Therefore, the higher mass groups may cover a wider variety of species. For example, the mass range of group 6, 190–625 amu/q, is much larger than the group 1 range of 12–30 amu/q. Hence, densities of one mass group compared to a different mass group could be higher simply because the mass range covered is broader.

[10] The largest random uncertainty in determining the densities is the subtraction of the background electrons. The uncertainty sources are electron anisotropies and inter-anode calibration uncertainties. The *reference density* (shown in Table 1) is a measure of this electron background subtraction uncertainty and was determined by a study that compares the observed electron background of different anodes. Negative ion densities above this value are considered real and can be used for scientific analysis; we estimate a 90% confidence that negative ion samples above the reference density are due to negative ions. They may not, however, be purely due to negative ions. A fraction of the processed counts may still be due to background electrons or inter-anode scaling uncertainties. The uncertainty due to these sources is given by the value of the reference density, and therefore, the percentage uncertainty due to these sources decreases with increasing density. The reference density can be used, for example, to determine the highest altitude at which a mass group is observed, which is shown in the right-hand column of Table 2.

3. Results and Discussion

[11] Figure 2 shows negative ion density versus altitude for the seven mass groups plus total density. The data are from 34 Cassini Titan encounters which make up 339 data points for each mass group. However, not all of the 339 data points per mass group are above the reference density (indicated by the vertical lines on the plots), and therefore, the number of data points that can be used scientifically varies with different mass groups as shown on the plots. One data point corresponds to one negative ion signature such as one of the spike-shaped structures in Figure 1. There are, on average, ten signatures per flyby. One signature lasts approximately 16 s. The altitudes shown in Figure 2 and discussed in the remainder of this paper are altitudes which correspond to the time stamp at the center of the ion signature. However, due to the approximately 16 s duration of the signatures, the selected data point (which is always the highest count rate of that signature) is not always at the center of the signature. The time stamp of the selected data point can also be different for different mass groups. Therefore, the given altitude has a maximum uncertainty of ±20 km. However, in most cases, the time stamp is on, or very close to, the central time stamp, and hence, for the majority of data points, the uncertainty is less than ±10 km.

[12] We can determine the altitude at which the maximum density is observed and the maximum altitude at which negative ions were detected above the reference density for each mass group. We refer to the latter altitude as the *reference altitude*; the corresponding data points are marked by an asterisk highlighted with a pink circle in Figure 2. This information is summarized in Table 2. We also show the

altitudes at which the density peaks during each of the 34 individual flybys for each mass group; these data points are marked by squares in Figure 2. The average of these local peak density altitudes for each mass group is shown in the column *peak average altitude* in Table 2 and is an average of the 34 peak densities. The vertical line near zero indicates the reference density. This value decreases with higher mass groups. Densities below the reference density are still shown but may not be real, especially values much lower than the reference density.

[13] The reference altitude decreases with increasing mass group. Hence, the upper altitude limit of where the different mass groups are observed decreases with increasing mass.

[14] The lowest observed densities at a specified altitude increase with decreasing altitude for mass groups 3 to 6. This happens quite abruptly in the case of group 4, where there is a lack of low densities below approximately 1050 km. The lowest densities of group 6 increase gradually with decreasing altitude. This trend only appears to occur from a certain altitude above which the lowest densities are close to the reference density; for example, in the case of group 6, this altitude is approximately 1060 km. The lowest densities at a specified altitude of groups 1, 2, and 7 remain close to the reference density at all altitudes.

[15] The highest observed densities at a specified altitude of all mass groups increase with decreasing altitude until altitudes near the peak average altitude are reached; the highest densities below this altitude tend to decrease with decreasing altitude. However, the latter trend becomes difficult to observe for the higher mass groups where the peak average altitude is closer to the CA (closest approach) altitudes and the peak may, especially in the case of group 7, be at a lower altitude. In addition, not all encounters studied in this work have CA altitudes near 950 km (see Table S1 in the supporting information); some CA altitudes are above 1000 km which means that the number of samples at the lowest altitudes is lower.

[16] The data points of the observed peak density for each individual flyby (marked by a square) tend to cover a relatively large-altitude range, especially at the lower masses, but they are generally clustered at lower altitudes. The averages of these peak density altitudes ("*peak average altitude*" shown in Table 2) decrease with increasing mass. During some flybys when CA was relatively high, the actual peak density may have been at a lower altitude than the recorded one because the spacecraft did not sample the lowest altitudes; hence, the values shown in Table 2 may be slightly higher than the real values.

[17] All mass groups except mass group 7 are observed during almost all encounters, provided that the flyby altitude is low enough and the instrument pointed in the ram direction. However, mass group 7 (625 amu/q and higher) ions are only sometimes observed even when the encounter is well below the reference altitude and below the peak average altitude. Mass group 7 therefore seems to be particularly dependent on other controlling factors in addition to the described altitude trend. Future studies will investigate possible factors controlling all mass groups including group 7.

[18] *Ågren et al.* [2012] report total negative ion densities in the range between $1000 \, cm^{-3}$ up to more than $10000 \, cm^{-3}/q$ at altitudes below 900 km during the T70 using RPWS/LP (Langmuir Probe) data. There are no CAPS-ELS data available from T70 because CAPS did not

point in the ram direction during this encounter. The lower limit of the *Ågren et al.* [2012] density range is close to the reported maximum total density of $948 \, cm^{-3}$ here. This could mean that total densities increase further at altitudes below 950 km. However, as stated above, uncertainties on the absolute values of densities in this study are large, and therefore, the reported densities by *Ågren et al.* [2012] are not necessarily higher. *Shebanits et al.* [2013] studied total negative ion densities using RPWS/LP data. The comparison between total densities of CAPS and LP data will be the focus of a future study.

[19] *Coates et al.* [2009] showed that the highest masses are observed at low altitudes. One difference between the density and maximum mass trends is that the density peaks seem to be reached above the lowest altitudes sampled (950 km), whereas the highest masses are observed at the very lowest altitudes. The peak densities of most of the individual mass groups occur at altitudes >950 km. This may be related to the ionospheric peak density observed in LP and Ion and Neutral Mass Spectrometer [see, e.g., *Coates et al.*, 2011, Figures 2–4].

4. Summary and Conclusions

[20] We show for the first time negative ion density trends of different mass groups with altitude in Titan's ionosphere. The data demonstrate that the highest densities are found at lower altitudes. The average altitudes where the peak densities occur decrease with increasing ion mass. In addition, the maximum altitudes at which ions from a specific mass group are observed (the *reference altitude*) decrease with increasing mass group. This study provides the first step in investigating the conditions which affect the densities of different negative ion mass groups using Cassini CAPS-ELS observations of Titan's ionosphere.

[22] The Editor thanks two anonymous reviewers for their assistance in evaluating this paper.

References

Ågren, K., N. J. T. Edberg, and J.-E. Wahlund (2012), Detection of negative ions in the deep ionosphere of Titan during the Cassini T70 flyby, *Geophys. Res. Lett.*, *39*, L10201, doi:10.1029/2012GL051714.

Borucki, W. J., R. C. Whitten, E. L. O. Bakes, E. Barth, and S. N. Tripathi (2006), Predictions of the electrical conductivity and charging of the aerosols in Titan's atmosphere, *Icarus*, *181*, 527–544.

Bruecken, S., H. Gupta, C. A. Gottlieb, M. C. McCarthy, and P. Thaddeus (2007), Detection of the carbon chain negative ion C8H- in TMC-1, *Astrophys. J.*, *664*, L43–46.

Chaizy, P., et al. (1991), Negative ions in the coma of comet Halley, *Nature*, *349*, 393–396.

Coates, A. J., F. J. Crary, G. R. Lewis, D. T. Young, J. H. Waite Jr., and E. C. Sittler Jr. (2007), Discovery of heavy negative ions in Titan's ionosphere, *Geophys. Res. Lett.*, *34*, L22103, doi:10.1029/2007GL030978.

Coates, A. J., A. Wellbrock, G. R. Lewis, G. H. Jones, D. T. Young, F. J. Crary, and J. H. Waite (2009), Heavy negative ions in Titan's atmosphere: Altitude and latitude dependence, *Planet. Space Sci.*, *57*(14–15), 1899–1871, doi:10.1016/j.pss.2009.05.00.

Coates, A. J., G. H. Jones, G. R. Lewis, A. Wellbrock, D. T. Young, F. J. Crary, R. E. Johnson, T. A. Cassidy, and T. W. Hill (2010a), Negative ions in the Enceladus plume, *Icarus*, *206*, 618–622, doi:10.1016/j.icarus.2009.07.013.

Coates, A. J., A. Wellbrock, G. R. Lewis, G. H. Jones, D. T. Young, F. J. Crary, J. H. Waite, R. E. Johnson, T. W. Hill, and E. C. Jr.Sittler (2010b), Negative ions at Titan and Enceladus: Recent results, *Faraday Discuss.*, *147*(1), 293–305, doi:10.1039/C004700G2010.

Coates, A. J., J.-E. Wahlund, K. Ågren, N. Edberg, J. Cui, A. Wellbrock, and K. Szego (2011), Recent results from Titan's ionosphere, *Space Sci. Rev.*, *162*, 85–111, doi:10.1007/s11214-011-9826-4, reprinted in The Plasma Environment of Venus, Mars and Titan, Space Sciences Series of ISSI, vol. 37, ed. K.Szego, 85–111.

Cravens, T. E., R. V. Yelle, J.-E. Wahlund, D. E. Shemansky, and A. F. Nagy (2010), Composition and structure of the ionosphere and thermosphere, in *Titan from Cassini-Huygens*, p. 259–295, edited by R. H. Brown, J.-P. Lebreton, and J. H. Waite, Springer, Dordrecht.

Fraser, G. W. (2002), The ion detection efficiency of microchannel plates (MCPs), *Int. J. Mass Spectrom.*, *215*, 13–30.

Hargreaves, J. K. (1992), *The Solar-Terrestrial Environment*, Cambridge Atmos. Space Sci. Ser., vol. 5, Cambridge Univ. Press, Cambridge, U. K.

Herbst, E. (1981), Can negative molecular ions be detected in dense interstellar clouds?, *Nature*, *289*, 656.

Hunten, D. M., M. G. Tomasko, F. M. Flasar, R. E. Samuelson, D. F. Strobel, and D. Stevenson (1984), Titan, in *Saturn*, p. 671, edited by T. Gehrels, and M. S. Matthews, Univ. of Arizona Press, Tucson.

Lavvas, P., et al. (2013), Aerosol growth in Titan's ionosphere, *Proc. Natl. Acad. Sci. U. S. A.,* in press.

Michael, M., S. N. Tripathi, P. Arya, A. Coates, A. Wellbrock, and D. T. Young (2011), High-altitude charged particles in the atmosphere of Titan, *Planet. Space Sci.*, *59*, 880–885.

Shebanits, O., J.-E. Wahlund, K. Mandt, K. Ågren, N. J. T. Edberg, and J. H. Waite Jr. (2013), Negative ion densities in the ionosphere of Titan–Cassini RPWS/LP results, *Planet. Space Science*, in press.

Sittler, E. C., Jr., A. Ali, J. F. Cooper, R. E. Hartle, R. E. Johnson, A. J. Coates, and D. T. Young (2009), Heavy ion formation in Titan's ionosphere: Magnetospheric introduction of free oxygen and a source of Titan's aerosols?, *Planet. Space Sci.*, *57*, 1547–1557, doi:10.1016/j.pss.2009.07.017.

Sittler, E. C., R. E. Hartle, C. Bertucci, A. J. Coates, T. E. Cravens, I. Dandouras, and D. Shemansky (2010), Energy deposition processes in Titan's upper atmosphere and its induced magnetosphere, in *Titan from Cassini-Huygens*, p. 393–453, edited by R. H. Brown, J.-P. Lebreton, and J. H. Waite, Springer, Berlin, doi:10.1007/978-1-4020-9215-2_16.

Vuitton, V., P. Lavvas, R. V. Yelle, M. Galand, A. Wellbrock, G. R. Lewis, A. J. Coates, and J.-E. Wahlund (2009), Negative ion chemistry in Titan's upper atmosphere, *Planet. Space Sci.*, *57*, 1558–1572.

Waite, J. H., D. T. Young, T. E. Cravens, A. J. Coates, F. J. Crary, B. Magee, and J. Westlake (2007), The process of tholin formation in Titan's upper atmosphere, *Science*, *316*(5826), 870–875, doi:10.1126/science.1139727.

Waite, J. H., D. T. Young, J. H. Westlake, J. I. Lunine, C. P. McKay, and W. S. Lewis (2010), High-altitude production of Titan's aerosols, in *Titan from Cassini-Huygens*, p. 201, edited by R. H. Brown, J.-P. Lebreton, and J. H. Waite, Springer, Dordrecht, doi:10.1007/978-1-4020-9215-2_8.

Young, D. T., et al. (2004), Cassini plasma spectrometer investigation, *Space Sci. Rev.*, *114*, 1–112, doi:10.1007/s11214-004-1406-4.